Calibration Process on the Study of New Antenna Array Architectures for Space Communications

Miguel A. Salas Natera, Ramón Martínez Rodríguez-Osorio, Leandro de Haro Ariet and Manuel Sierra Pérez.

{msalasn; ramon; leandro; m.sierra.perez}@gr.ssr.upm.es

Department of Systems, Signal and Radiocommunications
Grupo de Radiación, Universidad Politécnica de Madrid, Madrid, Spain

Abstract- **This paper introduces novel calibration processes applied to antenna arrays with new architectures and technologies designed to improve the performance of traditional earth stations for satellite communications due to the increasing requirement of data capacity during last decades. Besides, the Radiation Group from the Technical University of Madrid has been working on the development of new antenna arrays based on novel architecture and technologies along many projects as a solution for the ground segment in the early future. Nowadays, the calibration process is an interesting and cutting edge research field in a period of expansion with a lot of work to do for calibration in transmission and also for reception of these novel antennas under development.**

Keywords-component; antenna array; novel architectures; calibration process; errors; mutual coupling.

I. Introducción

The motivation of this work is based on the evaluation of new antenna technologies to improve the performance of traditional earth stations, regarding the increasing requirement of data upload and download capacity during last decades and launch of new mission [1,2,3]. These needs will be met with new technologies and new architectures of deep space [4], as well as for low earth orbit (LEO), medium earth orbit (MEO), and geostationary earth orbit (GEO) [5,6].

During the GEODA antenna development [7] about the design and prototyping of non-uniform adaptive antenna arrays for reception of meteorological signals at 1.7 GHz, the characterization, validation of sub-systems and calibration of an active antenna array demonstrator of the GEODA, shown in Fig 1, were proposed to be performed in laboratory and anechoic chamber facilities of the Radiation Group as part of the prototyping lifecycle. In recent efforts, GEODA system has been upgraded for transmission [8] demanding further analysis about On-site calibration techniques.

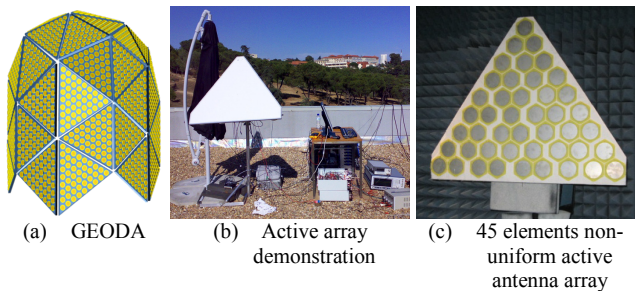| (a) GEODA | (b) Active array demonstration | (c) 45 elements non-uniform active antenna array |

Fig. 1. GEODA Antenna

The adaptive active antenna array under test uses adaptive beamforming algorithms based on spatial reference to track satellites. Thus, the compute of a close approach of the spatial reference as well the Direction of Arrival (DOA) estimation and the correct performance of the beamformer depends on the calibration results. Based on the research framework, motivation of this work, current systems, challenges and solutions given to the field of novel antenna array calibration and uplink arraying; a series of milestones are presented related to the calibration process and summarized in Fig 2. First, evaluation of errors based on the uncertainty analysis. Second, measurements for characterization and validation. Finally, the calibration process.
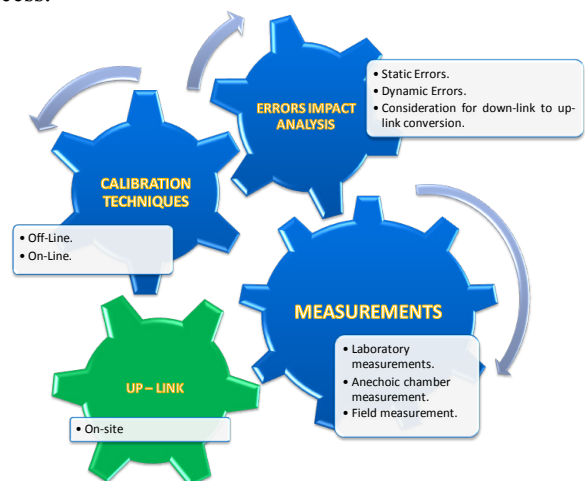

Fig. 2. Global calibration process diagram

This paper is organized as follows. Section II presents the experimental procedure. Section III introduces the uncertainty analysis. Section IV explains the proposed Off-line calibration procedure. Section V discusses important results. Finally, section VI draws significant conclusions.

II. Experimental procedure

The experimental procedure applied has four steps: Step 1, selection of the proper calibration technique based on the uncertainties analysis and mutual coupling evaluation; Step 2, evaluation of measurement requirements from the calibration technique to define the measurement campaign; Step 3, measurement procedure for measurement campaigns; and Step 4, post-processing of measurement results for

calibration and characterization. Table I presents a general measurement campaign to fulfill requirements of characterization, sub-system validation and calibration of a typical active antenna array design.

When the number of sub-systems and components symbolizes a challenge in terms of exhaustive, complex and expensive measurements campaign as those presented in Table I, and automated system is required for cost reduction during this process. This paper presents only some significant results of the work carried out and the measurement campaign done for characterization, validation of sub-systems and calibration of one active antenna array of the GEODA.

TABLE I.

TESTS FOR MEASUREMENT CAMPAIGN

Test	Output	Facility	Equipments
1	Coupling coefficient of the antenna array.		Vector Network Analyzer. VNA Calibration Kit. Antenna worksatetion. RF Connectors and waveguides. Power supply device.
2	S21 parameters of branches of RF circuits.	Laboratory measurements	
3	S21 parameters of branches of RF complete network (No hybrid couplers included).		
4	Active element patterns of sub-arrays and complete antenna array pattern.	Anechoic Chamber measurements	Anechoic Chamber of the certified Laboratory of Tests and Standardization of Antennas (LEHA). Antenna Workstation. RF Connectors and waveguides. Power supply device.

III. UNCERTAINTY ANALYSIS

The effect of errors on the antenna array response has been well analyzed based on a proposed signal model for active antenna arrays with Monte Carlo simulation. As outcome of this study, a novel analytical method for uncertainty evaluation in active antenna arrays is proposed in [9], and the complete expansion of the analytical model demonstrated. The aim of this analytical method in equation (1) is to analyze the impact of amplitude, phase and sensor location errors on the array response.

$$U(\theta,\varphi) = 1 + K_p \left[\begin{array}{c} +(-u^2(\Psi)) \\ +(u^2(G_{RF})) \\ +\left(-u(\vec{r})\frac{2\pi}{\lambda}(\sin\theta\cos\varphi + \sin\theta\sin\varphi + \cos\theta)\right)^2 \end{array} \right]^{1/2} \quad (1)$$

Where G_{RF}, Ψ and $\vec{r}$ are the Gain, Phase and Location uncertainty sources, respectively. The standard uncertainty $u(x_l)$ which is the estimated standard deviation of the mean value, associated to the l th input quantity x_l, whose values are estimated from Q independent observations $X_{l,k}$ of X_l under the same measurement conditions, can be computed as

$$u(x_l) = \left[\frac{1}{Q(Q-1)} \sum_{k=1}^{Q} (X_{l,k} - \bar{X}_l)^2 \right]^{1/2} \quad (2)$$

Main applications of the analytical method for uncertainty evaluation are: analytical evaluation of uncertainty in the complete array response for design and selection of the proper calibration technique of active antenna arrays, and analysis for the components selection during prototyping and design. This method for evaluation offers a significant reduction in computational complexity and time as compared to Monte Carlo simulations. Using the analytical equation instantaneous results are obtained, while

with Monte Carlo simulation depending on the number of data to be evaluated and the hardware for computation available, these simulations can require several minutes as well as a complete day.

IV. OFF-LINE CALIBRATION

In this work, we deal with the problem of calibration of active antenna arrays at reception. The definition of the Off-line calibration process is presented in Fig 3 as a part of the experimental procedure for characterization and calibration. Note that for calibration purposes only tests 3 and 4 of Table 1 are recommended.

Next, the active antenna array pattern model for the expansion of equation for calibration is presented, followed by the derived expression of the active element pattern and the cost function including gain and phase errors, and mutual coupling effect.
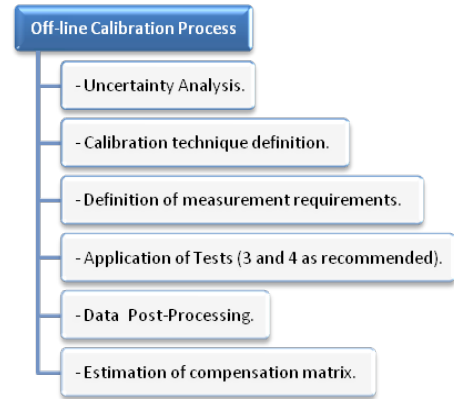

Fig. 3. Flowchart of the Off-line calibration

A. Active Antenna Array Pattern Model

The active array pattern $Y(\theta,\varphi)$ including modeling errors can be expressed as

$$Y(\theta,\varphi) = \underline{W}^H \underline{M}(\theta,\varphi) \quad (3)$$

Where $\underline{W}$ represents the beamforming vector whose m-th term represents the complex beamforming weight for the m-th antenna element and $(\cdot)^H$ is the Hermitian operator. $\underline{W}$ can be computed to synthesize an antenna pattern that satisfies an optimization criterion, such as tracking of moving targets, cancellation of interference sources, etc.. $\underline{M}(\theta,\varphi)$ is the array manifold that includes the error contributions and can be expressed as

$$\underline{M}(\theta,\varphi) = C(G_{RF} + \Delta G_{RF}) \cdot \left(\underline{G}(\theta,\varphi) + \underline{\Delta G}(\theta,\varphi) \right) \odot \left(\underline{A}(\theta,\varphi) + \underline{\Delta A}(\theta,\varphi) \right) \quad (4)$$

$\underline{M}(\theta,\varphi)$ is a $M \times 1$ vector that can be denoted as $[M_1 \ M_2 \ \cdots \ M_M]^T$, whose m-th vector element is a $\theta \times \varphi$ matrix. The $\odot$ represents the Hadamard product, C is a $M \times M$ matrix that represents the mutual coupling; G is a $M \times 1$ vector representing the gain $\underline{g}$ and phase $\underline{\phi}$ as $\underline{g}_m e^{j\underline{\psi}_m}$ of the m-th $\theta_n \times \varphi_n$ matrix.; A is a $M \times 1$ vector representing the ideal steering vector of the array as $A = e^{-j\frac{2\pi}{\lambda}\vec{r}\hat{r}'}$, being $\vec{r}$ the array location vector, $\hat{r}'$ is the unitary direction vector in (θ,φ), $\hat{r}' = [(\sin\theta\cos\varphi \ \sin\theta\sin\varphi \ \cos\theta)]^T$, and λ is the wavelength. ΔG and $\Delta \underline{A}$ are the deviation of G and A due to the presence of errors, respectively, whose m-th vector element is a $N \times N$ matrix.

Note that in case with no errors and noise, the expression for the ideal beamformed array pattern $Y_o(\theta,\varphi)$, can be rewritten as

$$Y_o(\theta,\varphi) = \underline{W}_o^H \left(C G_{RF} \underline{G}(\theta,\varphi) \odot \underline{A}(\theta,\varphi) \right) = \underline{W}_o^H \underline{M}_o(\theta,\varphi) \tag{5}$$

B. Active Element Pattern Model

Since the fully excited antenna array can be expressed in terms of the active element pattern and the array factor, the active element pattern is useful in the characterization of an antenna array. Furthermore, the scattering matrix can be computed from the active element patterns [10,11]. The radiated electric field of the m-*th* active element can be written as presented in equation (6).

With the active element pattern of the M elements measured for broadside, it is possible to compute the scattering matrix evaluating the active pattern. Following, in equation (7) the expression for the active element pattern of the m-*th* element of the array is presented.

$$E_m = E_e(\theta_n, \varphi_n) V_o \cdot$$
$$\left[\begin{array}{c} e^{-jk_o(dx_m \sin\theta_0 \cos\varphi_0 + dy_m \sin\theta_0 \sin\varphi_0)} \\ + \sum_{k=1}^{K} S_{km} e^{-jk_o(dx_k \sin\theta_0 \cos\varphi_0 + dy_k \sin\theta_0 \sin\varphi_0)} \end{array} \right] \cdot \tag{6}$$
$$e^{jk_o(dx_m \sin\theta_n \cos\varphi_n + dy_m \sin\theta_n \sin\varphi_n)}$$

$$E_m(\theta_n, \varphi_n) = E_e(\theta_n, \varphi_n) e^{jk_o(\mu_n(m) - \mu_o(m))} [1 + \underline{S}_{mk} \underline{D}_{mk}] \tag{7}$$

Where $\underline{S}_{mk} = [S_{m1} \quad S_{m2} \quad \cdots \quad S_{mK}]$ is the vector of scattering coefficients of the m-*th* antenna element. D_{mk} is the phase differences matrix due to the location of the k-*th* neighbor element related to the m-*th* element. The $K \times 1$ vector $\underline{D}_{mk}$ for $k = 1,2,\ldots,K$ can be expressed as $[e^{-jk_o(\mu_o(1)-\mu_o(m))} \quad e^{-jk_o(\mu_o(2)-\mu_o(m))} \quad \ldots \quad e^{-jk_o(\mu_o(K)-\mu_o(m))}]^T$. $\mu_o(m)$ and $\mu_n(m)$ represent the phase of the m-*th* element for the broadside measured angle and the evaluating point angle, respectively. Thus, $e^{jk_o(\mu_n(m)-\mu_o(m))}$ can be written as R expressed as follows

$$R = e^{jk_o(\mu_n(m) - \mu_o(m))} = e^{j\left(\frac{2\pi}{\lambda}\right)\vec{r}_m \hat{r}_n'} \cdot e^{-j\left(\frac{2\pi}{\lambda}\right)\vec{r}_m \hat{r}_o'} \tag{8}$$

Ehe equation (7) can be written as

$$E_m(\theta,\varphi) = E_e(\theta,\varphi) \odot R [1 + \underline{S}_{mk} \underline{D}_{mk}] \tag{9}$$

The term E_i can be introduced as the isolated element pattern including its location at the array geometry expressed by $E_i = E_e \odot Rp$ to simplify equation (9). Furthermore, for (θ_0, φ_0) where $\underline{S}_{mk} \underline{D}_{mk}$ can be direct estimated, the active element pattern can be expressed as

$$E_m(\theta_0, \varphi_0) = E_i(\theta_0, \varphi_0) [1 + \underline{S}_{mk} \underline{D}_{mk}] \tag{10}$$

C. Estimation of Compensation Matrices

The theory for the estimation of a complete compensation matrix including mutual coupling effect, phase and gain error is addressed in this section. Regarding equation (4), a new term for a general approximation of errors can be included expressed.

$$M_e(\theta,\varphi) = C \left(\Delta G_{RF} \Delta G(\theta,\varphi) \Delta A(\theta,\varphi) \right) \tag{11}$$

Where $M_e(\theta,\varphi)$ is the general matrix of errors and mutual coupling of the array manifold. Coefficients of $M_e(\theta,\varphi)$ include amplitude and phase contribution of uncertainties and coupling coefficients. When active element patterns are measured with RF circuit assembled, errors due to dissimilar branches of RF circuits, are included in $M_e(\theta,\varphi)$. Regarding this, the array manifold can be written as

$$\underline{M}(\theta,\varphi) = M_e(\theta,\varphi) \, G_{RF} \left(\underline{G}(\theta,\varphi) \odot \underline{A}(\theta,\varphi) \right) \tag{12}$$

The amplitude $|M_e|$ of coefficients of the matrix $M_e(\theta,\varphi)$ defined in terms of the array gain uncertainty matrix, the gain uncertainty diagonal matrix of RF circuits and the mutual coupling can be expressed as

$$|M_{e(m,k)}| = |1 + S_{mk} D_{mk}| \, \Delta G_{RF_m} \, \Delta G_m(\theta,\varphi) \tag{13}$$

The phase $e^{j\left(\frac{2\pi}{\lambda}\right)\overrightarrow{\Delta r}_m \hat{r}_n'}$ of coefficients of the matrix $M_e(\theta,\varphi)$ defined in terms of the phase uncertainty of sensors location $\left(e^{j\left(\frac{2\pi}{\lambda}\right)\overline{\delta r}\hat{r}_n'}\right)$, array phase uncertainty $\left(e^{j\left(\frac{2\pi}{\lambda}\right)\Delta\psi_m(\theta,\varphi)}\right)$, phase uncertainty of RF circuits $\left(e^{j\left(\frac{2\pi}{\lambda}\right)\Delta\psi RF_m(\theta,\varphi)}\right)$ and the mutual coupling $\left(e^{j\left(\frac{2\pi}{\lambda}\right)(\vec{r}_m - \vec{r}_K)\hat{r}_o'}\right)$ can be expressed as follows

$$e^{j\left(\frac{2\pi}{\lambda}\right)\overrightarrow{\Delta r}_m \hat{r}_n'}{}_{(m)} = e^{j\left(\frac{2\pi}{\lambda}\right)\overline{\delta r}\hat{r}_n'} \, e^{j\left(\frac{2\pi}{\lambda}\right)\Delta\psi_m(\theta,\varphi)} \cdot$$
$$e^{j\left(\frac{2\pi}{\lambda}\right)\Delta\psi RF_m(\theta,\varphi)} \, e^{j\left(\frac{2\pi}{\lambda}\right)(\vec{r}_m - \vec{r}_K)\hat{r}_o'} \tag{14}$$

Amplitude and phase of coupling coefficients can be modeled based on the scan reflection coefficient [10], where the phase $\left(\frac{2\pi}{\lambda}\right)(\vec{r}_m - \vec{r}_K)\hat{r}_o'$ is the result of the phase of the m-*th* element of the array plus the sum of coupled contributions from its K neighbors as follow

$$|1 + S_{mk} D_{mk}| \, e^{j\left(\frac{2\pi}{\lambda}\right)(\vec{r}_m - \vec{r}_K)\hat{r}_o'} =$$
$$\left[\begin{array}{c} 1 + e^{jk_o(dx_m \sin\vartheta_0 \cos\varphi_0 + dy_m \sin\vartheta_0 \sin\varphi_0)} \cdot \\ \sum_{k=1}^{K} S_{mk} e^{-jk_o(dx_k \sin\vartheta_0 \cos\varphi_0 + dy_k \sin\vartheta_0 \sin\varphi_0)} \end{array} \right] \tag{15}$$

Based on the statement commented above, equation (14) provides the phase center shift $\overrightarrow{\Delta r}$ of the m-*th* element of the array. To estimate the matrix $M_e(\theta,\varphi)$ it is possible to evaluate the equation (12) using at least square matrix inversion.

$$\min_{M_e(\theta,\varphi)} \left\| \underline{M}(\theta,\varphi)^T - \left[G_{RF} \left(\underline{G}(\theta,\varphi) \odot \underline{A}(\theta,\varphi) \right) \right]^T M_e(\theta,\varphi) \right\|_2^2 \tag{16}$$

The least squares solution is the matrix $M_e(\theta,\varphi)^T$ which include the unknown vector of coefficients. The normal system of equations using the transpose of each vector of equation (16) is given by

$$\left(\left[G_{RF} \left(\underline{G}(\theta,\varphi) \odot \underline{A}(\theta,\varphi) \right) \right] \left[G_{RF} \left(\underline{G}(\theta,\varphi) \odot \underline{A}(\theta,\varphi) \right) \right]^T \right) M_e(\theta,\varphi) =$$
$$\left[G_{RF} \left(\underline{G}(\theta,\varphi) \odot \underline{A}(\theta,\varphi) \right) \right] \underline{M}(\theta,\varphi)^T \tag{17}$$

Finally, the solution for $M_e(\theta,\varphi)$ can be expressed as

$$M_e(\theta,\varphi) = \left(\left[G_{RF} \left(\underline{G}(\theta,\varphi) \odot \underline{A}(\theta,\varphi) \right) \right] \left[G_{RF} \left(\underline{G}(\theta,\varphi) \odot \underline{A}(\theta,\varphi) \right) \right]^T \right)^{-1}$$
$$\left[G_{RF} \left(\underline{G}(\theta,\varphi) \odot \underline{A}(\theta,\varphi) \right) \right] \underline{M}(\theta,\varphi)^T \tag{18}$$

V. RESULTS

Laboratory and anechoic chamber measurements have been performed to complete the measurement procedure. Furthermore, implementing an automated procedure supported by the control system of the GEODA antenna and the control system of the anechoic chamber, an important reduction of about 900 hours of tests was obtained. The group of tests explained have been executed as a sequence and some of the more relevant results are presented in this discussion. For the test 2, it was necessary to carried out

4860 measurements of the S21 parameter to evaluate 6 states of phase-shifters and 3 states of LNA of patches.

From Test 4, Figure 7 depicts the normalized pattern of the triangular active array pointing to θo = 30º, φo = 0º at f = 1.7 GHz, and the active array has a gain losses due to the miss-pointing about 1.5 dB which means a pointing error about 5º for the 30º pointing direction pattern presented due to the presence of errors and mutual coupling.

Fig 5 shows good results of the application of the compensation matrix obtained from equation (18) using one sub-array of 4 cells of the antenna array in Fig 1.(c) and measurements from Test 4 for validation of the Off-line calibration proposal. Furthermore, Fig 5 presents the pattern of the sub-array under evaluation based on the isolated pattern as well as the pattern based on measured active element patterns of patches under test.
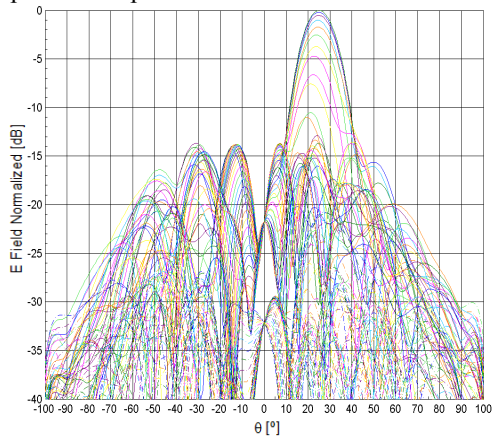

Fig. 4. Anechoic chamber measurement of the pattern of the triangular active array panel at θo = 30º, φo= 0º and f = 1.7 GHz
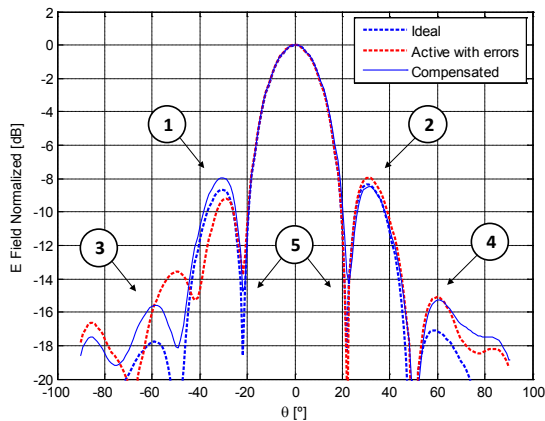

Fig. 5. Comparison curve for the sub-array of 4 cells

Additionally, Fig 5 shows main points highlighted where compensated pattern presents about -8 dB of side-lobe in point 1, and for point 2 has –8.5 dB, as well as the ideal pattern. Regarding side-lobes in points 3 and 4, the Compensated pattern has a considerable reduction of about 2 dB with respect of Active pattern with errors. As conclusion, compensated pattern is more symmetrical than active pattern (before compensation), and presents a good performance in terms of compensation of the complete pattern.

VI. Conclusions

In this work an experimental procedure to achieve the calibration schedule and characterization of active antenna arrays based on the experience with the characterization, analysis and estimation of compensation matrices during the study of new calibration procedures done to one panel array of the GEODA, and the accompanying automated measurements implementation, have been presented. Although methods has focused on active antenna arrays it can be applied to any other antenna.

For calibration purposes, only Test 3 and 4 are recommended reducing the measurements about 73% in time and cost. Test 4 can be reduced only to the measurement of active element pattern of cells. Furthermore, active element pattern of patches and different pointing direction measurements can be done just for validation of mutual coupling model and sub-systems if required.

The proposed experimental procedure for calibration process is presented from a system level framework, including measurements as an essential part in the process leading to the calibration and characterization of the array. Using the proposed Off-line calibration algorithm to estimate the matrix $M_e(\theta, \varphi)^T$, good results in terms of reduction of errors were obtained and a reduction in measurement time is achieved thus reducing the operational costs for the calibration of active antenna arrays when measuring active cell patterns only.

References

[1] F. Davarian, "Uplink Arrays for the Deep Space Network," *Proceedings of the IEEE*, vol. 95, no. 10, pp. 1923-1930, Oct. 2007.

[2] B. J. Geldzahler, J. J. Rush, and L. J. Deutsch, "Engineering the Next Generation Deep Space Network," in Proc. *IEEE - MTT-S International Microwave Symposium*, Honolulu, HI, June 2007, pp. 931-934.

[3] F. Amoozegar, L. Paal, A. Mileant, and D. Lee, "Analysis of Errors for Uplink Array of 34-m Antennas For Deep Space Applications," in Proc. *2005 IEEE Aerospace Conference*, Big Sky, Montana, March 2005, pp. 1235-1257.

[4] J. C. I. o. Technology. (2010, Mar.) Deep Space Network Brochure. [Online]. http://deepspace.jpl.nasa.gov/dsn/brochure/

[5] R. Martínez and M. A. Salas Natera, "On the use of Ground Antenna Arrays for Satellite Tracking: Architecture, Beamforming, Calibration and Measurements," in Proc. *61st International Astronautical Congress*, Prague, 2010, pp. 1-7.

[6] M. A. Salas Natera, A. García Aguilar, J. Mora Cuevas, J. M. Fernández, P. Padilla de la Torre, J. García-Gasco Trujillo, R. Martínez Rodríguez-Osorio, M. Sierra-Pérez, L. De Haro Ariet, and M. Sierra Castañer, "New Antenna Array Architectures for Satellite Communications," in *Advances in Satellite Communications*. InTech, 2011, ch. 7, pp. 167-194.

[7] M. Sierra Pérez, A. Torre, J. L. Masa Campos, D. Ktorza, and I. Montesinos, "GEODA: Adaptive Antenna Array for Metop Satellite Signal Reception," in Proc. *4th ESA International Workshop on Tracking, Telemetry and Command System for Space Application*, Darmstadt, September 2007, pp. 1-4.

[8] M. Arias Campo, I. Montesinos Ortego, J. L. Fernández Jambrina, and M. Sierra Pérez, "GEODA – GRUA: Diseño del módulo T/R," in Proc. *XXIV Simposium Nacional de la Unión Científica de Radio*, Santander, Septiembre 2009, pp. 115-116.

[9] M. Salas Natera and R. Martínez, "Analytical Evaluation of Uncertainty on Active Antenna Arrays," *IEEE Transactions on Aerospace and Electronic Systems*, vol. 48, No. 3, July 2012.

[10] D. M. Pozar, "A relation between the active input impedance and the active element pattern of a phased array," *IEEE Transactions on Antennas and Propagation*, vol. 51, no. 9, pp. 2486-2489, Sep. 2003.

[11] D. M. Pozar, "The Active Element Pattern," *IEEE Transactions on Antennas and Propagation*, vol. 42, no. 8, pp. 1176-1178, Aug. 1994.